Microelectronic Engineering 113 (2014) 35–39

Contents lists available at SciVerse ScienceDirect

Microelectronic Engineering

journal homepage: www.elsevier.com/locate/mee

Accelerated Publication

Deep reactive ion etching of sub-micrometer trenches with ultra high aspect ratio

Jayalakshmi Parasuraman [a], Anand Summanwar [b], Frédéric Marty [a], Philippe Basset [a], Dan E. Angelescu [a], Tarik Bourouina [a,*]

[a] Université Paris-Est, ESYCOM Lab EA 2552, ESIEE Paris, Cité Descartes-2, Bd Blaise Pascal, F-93162 Noisy-le-Grand, France
[b] SINTEF, ICT Microsystems & Nanotechnology, Gaustadalléen 23C0373, Oslo, Norway

ARTICLE INFO

Article history:
Received 4 February 2013
Received in revised form 2 June 2013
Accepted 21 June 2013
Available online 17 July 2013

Keywords:
DRIE
Bosch process
Cryogenic process
High aspect ratio
Sub-micrometer
MEMS

ABSTRACT

This paper focuses on deep reactive ion etching (DRIE) of sub-micrometer features. Very high aspect ratios up to 160:1 on trenches of 250 nm have been achieved using the Bosch process and up to 120:1 on trenches of 35 nm using a cryogenic process. The proposed etch recipes are specifically optimized for sub-micrometer features, and are not compatible with feature sizes in the tens of micrometer range. Based on analyzing data from our experiments and from literature, we show that a previously reported two-parameter empirical logarithmic law accurately describes the dependency of aspect ratio on trench width over a wide range of widths and etch parameters, including the sub-micrometer regime. We also propose a new figure of merit (FOM) that describes the ultimate aspect ratio achievable for any given etching process. This FOM also allows comparison of different aspect ratio performances, while taking into account in the same time, the dimension of the trench for which this performance is attained.

1. Introduction

Deep reactive ion etching (DRIE), initially developed for silicon-based MEMS, is gaining increasing interest in a much wider area of applications in the semiconductor industry. Besides MEMS, the other main drivers of this growth of DRIE include advanced packaging [1], power electronics [2], passive capacitive components [3], complex microfluidics devices [4], and micro-optics [5]. For most applications of DRIE, the main concern is in achieving trenches of very high aspect ratio: increasing the aspect ratio enables increasing the number of through-silicon-vias (TSVs) of a packaging layer, the electrostatic force of a MEMS actuator, and the highest achievable capacitance of a micro-machined passive component, respectively. For devices at the scale of tens of micrometers, adequate processes exist which cover the common industry needs. However, when considering sub-micrometer features, there is still a significant margin of progress that can be achieved. This is certainly the case for the above-mentioned capacitive devices [3] or for certain photonics applications, where high aspect ratio (HAR) features of quarter-wavelength width can lead to better quality Bragg mirrors [5]. HAR structures are also explored for producing thermoelectric meta-materials based on vertical superlattices [6], and highly electromagnetic-absorbent surfaces for solar cells [7]. In all these applications, the aspect ratio is the relevant figure of merit governing the ultimate performance of the devices.

On the other hand, there is no clear quantitative figure of merit which can be used to characterize the ability of a given etch process to produce HAR structures, and thus to assist the user in the selection of the most appropriate process. Usually, one of two forms of the DRIE process are used in HAR etching – the "Bosch" process on one hand, which is based on alternating depassivation, etch and repassivation steps [8], and the cryogenic process on the other hand, which involves etching at temperatures, typically below −100 °C [9]. Both have enjoyed success at etching micrometer and sub-micrometer features to great depths. Using the Bosch process, very high aspect ratio trenches have been reported in literature. Trenches with aspect ratios of up to 107:1 were reported for 374 nm widths by Marty et al. [10]. More recently, aspect ratios of 97:1 have been reported by Owen et al. [11] for trenches of 3 μm widths. Other results have been published for trenches ranging from 130 nm to 2.3 μm, where aspect ratios between 30:1 and 60:1 [12,13] were achieved. When considering cryogenic etching results, aspect ratios of 47.5:1 have been reported by Tillocher et al. [14] using STiGer cryoetching process.

In this manuscript, we describe optimized Bosch processes to fabricate very deep silicon trenches with aspect ratios of 160:1 for trenches of 250 nm widths, and of 124:1 for trenches of

* Corresponding author. Address: ESIEE Paris, Bd Blaise Pascal, Noisy le Grand 93162, France. Tel.: +33 (0) 1 4592 6692 (O); fax: +33 (0) 1 4592 6699.
E-mail address: t.bourouina@esiee.fr (T. Bourouina).

0167-9317/$ - see front matter © 2013 Elsevier B.V. All rights reserved.
http://dx.doi.org/10.1016/j.mee.2013.06.010

Table 1
Parameters for deep etching of sub-micron features using Bosch process (Set 1 and Set 2).

(a) General parameters

	Source power (W)	Pressure (mT)	Temperature (°C)	Duration (s)	Etch rate (μm/min)
Set 1	2800	25-50	10	6610	0.90
Set 2	1800	30	20	3600	0.66

(b) Specific parameters for the passivation pulse

	C_4F_8 flow (sccm)	RF power (W)	Pulse duration (s)
Set 1	350	30	2,4
Set 2	200	100	2

(c) Specific parameters for the etching and depassivation pulse

	SF_6 flow (sccm)	RF power (W)	Pulse duration (s)
Set 1	300	See figure below	See figure below
Set 2	300	100	5

(d) Detailed ramped parameters used in set 2 for RF power and pulse duration

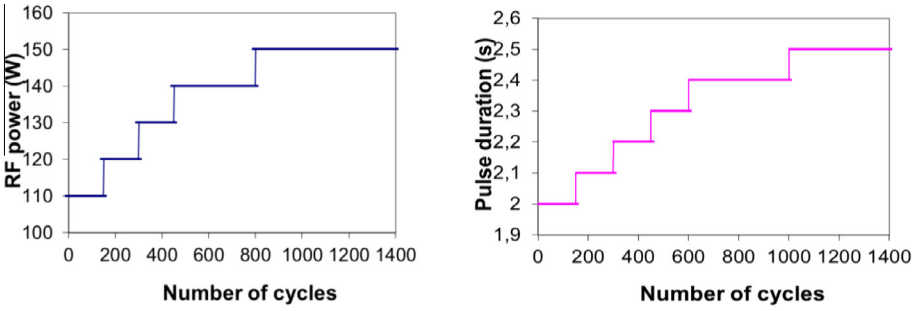

800 nm widths respectively. Furthermore, we show preliminary results suggesting that cryogenic etch processes can be used to produce aspect ratios greater than 120:1 for 35 nm trenches. To the authors' knowledge, these are the highest values of the aspect ratio attained so far using DRIE in these dimension ranges. By combining our experiments with other reports published in the literature, we show that the dependence of aspect ratio on feature width obeys a simple two-parameter logarithmic law for a wide range of process parameters and dimensions, allowing us to propose a new figure of merit to characterize the ultimate aspect ratio that can be obtained using a specific etch process. This figure of merit also allows achieving comparison of different aspect ratio performances, while taking into account in the same time, the dimension of the trench for which this performance is attained.

2. Etching experiments

2.1. Bosch process etching

The basic Bosch process is a time-multiplexed plasma etch process typically involving three distinct steps that alternate – depassivation, etch and repassivation. Some steps maybe performed concurrently. To overcome the problem of excess bowing at the top of the trenches and of narrowing at the bottom, numerous etch trials accompanied by a detailed study of the relationship between the three etch steps were performed. The best etch profile was obtained using a two-step process in which the depassivation and the etching were combined in one step. Since silicon etching takes place in this case at a lower pressure than in the regular Bosch process, this leads in a decrease of both etch rate and selectivity. Two sets of experiments were performed with the optimized Bosch process. An Aluminum layer of 500 nm thickness was evaporated as a masking layer for the extremely high selectivity it offers during the DRIE process (>300:1). The etch processes were performed on an Alcatel AMS200SE machine. Set 1 constitutes simple trench test structures of 800 nm width, whereas Set 2 consists of trenches increasing in width from 250 nm to 5 μm, with spacing of ~250 nm between them. Both were fabricated on standard <100> p-doped silicon (from Ultrasil – resistivity 0.01–0.015 Ω-cm). The detailed etch programs used for the two experiments are shown in Table 1, and the obtained results are represented in Fig. 1. Using the Set 1 etching conditions in Table 1, 800 nm-wide trenches with extremely vertical profiles and no bowing were manufactured, reaching aspect ratios as high as 124:1 (Fig. 1a). When considering the aspect ratio quantitatively, a decrease in feature size can lead to higher aspect ratios. Achieving an aspect ratio of 124:1 on trenches as wide as 800 nm-wide trenches is therefore a challenge, requiring dynamic adjustments of both the duration of the steps and of the plasma power for Set 1. It is also to be noted that the DRIE process is self-limiting due to the decrease in etch rate from radical depletion described by the Knudsen transport model [15], ion depletion due to sidewall scattering, electrostatic deflection and angular distribution [16]. Yeom et al. [17] also describe a *critical aspect ratio*, corresponding to the ultimate aspect ratio that can be achieved by a process upon saturation and it turns to be no longer dependent on the etch duration. It is therefore reasonable to assume that any recipe of DRIE process has a maximum achievable aspect ratio. Using the Set 2 etch conditions in Table 1, the highest aspect ratio was obtained for the 250 nm-wide trenches. The etch extended 40 μm in depth, resulting in an extremely high aspect ratio, of 160:1. The post-etch dicing of the samples for the purpose of SEM observation resulted in collapsed walls, as apparent in Fig. 1, however the effectiveness of etch is apparent from the regular square profile at the bottom of the trenches, which also suggests that even higher aspect ratios might be possible by further etching, as the saturation is not yet reached in this case.

Bosch process DRIE is also known to result in scalloping in the form of quasi-periodic sidewall roughness. Typical Bosch process surface roughnesses are in excess of 200 nm. However, when considering small trenches (in the range below 5 μm) and certainly like those used in our Set 1 & 2 experiments, this roughness drastically reduces to levels below 25 nm as roughly estimated from Fig. 1.c. This roughness eventually vanishes with increasing aspect ratios during the process, as detailed in a previous report [18],

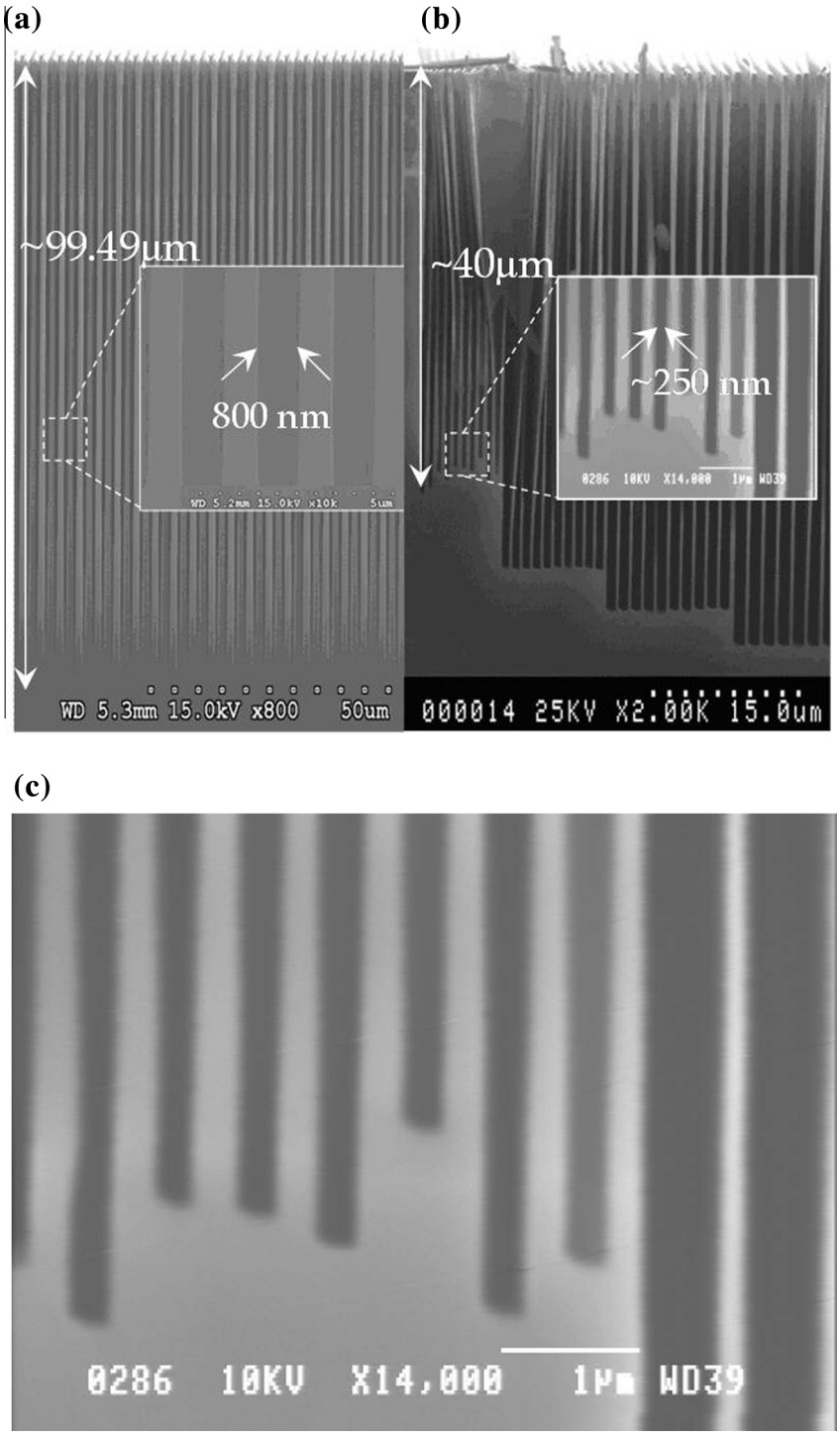

Fig. 1. High aspect ratio (HAR) structures manufactured using the Bosch process: (a) 800 nm-wide trenches with a depth of 99.5 μm (aspect ratio 124:1) and (b) 250 nm-wide trenches with a depth of 40 μm (aspect ratio 160:1). Some of the walls collapsed during the dicing procedure. (c) Is a magnified view of the inset shown in (b).

Table 2
Process parameters for the cryogenic etch process (Set 3).

Source Power (W)	SF6 flow (sccm)	O_2 flow (sccm)	Pressure (mT)	Substrate bias (W)	Temp (°C)	Duration of etch (min)	Etch rate (μm/min)
1000	200	12	30	80	−110	10	0.45

which indicates that surface roughness induced by the cyclic nature of the Bosch process, is significantly attenuated when increasing the aspect ratio of deep trenches, which is especially true for the sub-micron trenches under consideration in the present work, whose aspect ratio is extremely high, leading to non-observable surface roughness.

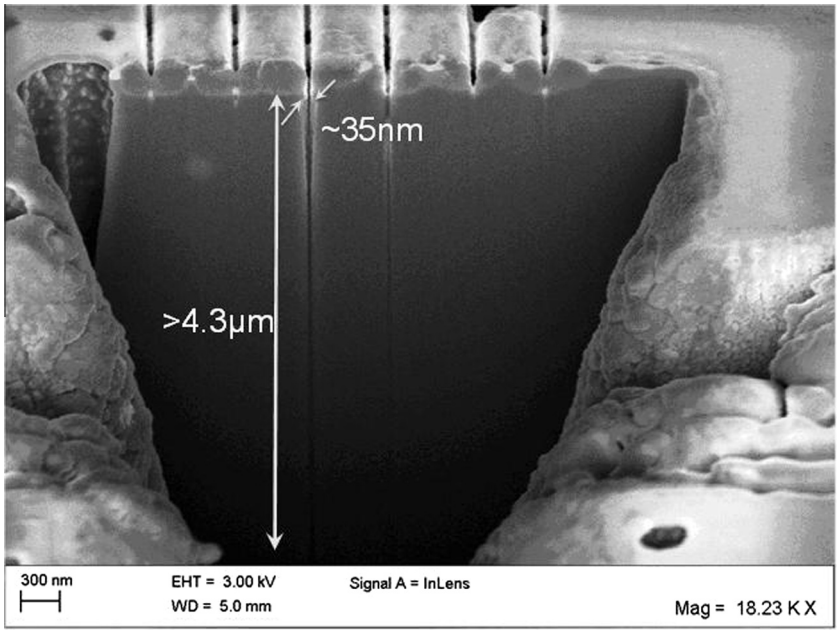

Fig. 2. Scanning electron microscope (SEM) image of a 35 nm-wide trench etched to a depth greater than 4.3 μm, hence with aspect ratio of more than 125:1. A rectangular hole was etched using the FIB to allow cross-sectional visualization.

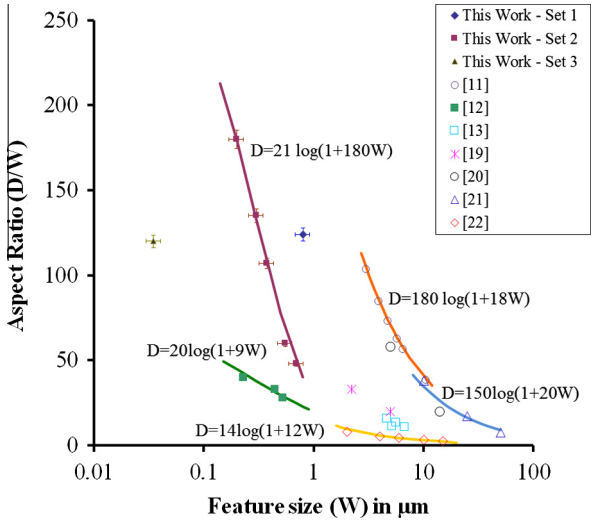

Fig. 3. Aspect ratio versus feature size as studied by various groups for feature sizes ranging from tens of nanometers up to tens of micrometers. All data are found to fit well with the proposed two-parameter logarithmic law of Eq. (1).

2.2. Cryogenic DRIE

By comparison with the Bosch process, which is known to produce a periodic roughness of typically tens of nanometers peak-to-valley, cryogenic DRIE offers the benefit of producing vertical sidewalls with no observable roughness. This advantage of the cryogenic process is of great significance, especially when etching sub-micrometer structures. This is a consequence of the process being carried out at extremely low temperatures using a plasma of combined sulfur hexafluoride (SF_6) and oxygen (O_2), and results in efficient reduction of the isotropic etching of silicon.

The challenge in case of cryogenic etches is to use a suitable mask that will resist at such temperatures and that can be patterned at sub-micrometer length scales. Typical photoresist masks peel off without being able to withstand cryogenic temperatures and were therefore considered unsuitable. For the final set of experiments performed in this work (Set 3), we used a combination of focused ion beam (FIB) etching and cryogenic DRIE to achieve HAR trenches with widths in the tens of nanometers range. The FIB was used to pattern lines of 35 ± 10 nm width and 500 nm spacing on a 70 nm-thick aluminum film. This created a hard mask for the subsequent etching, which used the process parameters shown in Table 2. All etching experiments were performed on an Alcatel 601E machine which is equipped with a cryogenic chuck. Samples were mounted on top of sacrificial test wafers deposited with aluminum using high vacuum grease. Fig. 2 shows the corresponding SEM results, indicating that aspect ratios of >125:1 could be achieved. We also note that the FIB was used again, before the imaging, to etch a vertical rectangular hole that exposes a partial cross-sectional view of the etching.

When compared to the Bosch process described in the previous section, it can be noted that it is performed at almost twice the bias at which the cryogenic process is performed. This can be explained by the fact that the Al mask thickness for the Bosch process is of the order of 500 nm as compared to only 70 nm for the cryogenic process. In the latter, we lower the ion bombardment to avoid any damage (or sputtering) to the Al layer while maintaining enough energy to penetrate to the bottom of the trench. As for why this difference in terms of ion bombardment between Bosch and cryogenic process is needed, it is perhaps possible to link it to the passivation layer itself and the fact that we compare a process with a dedicated passivation step (Bosch process) to a continuous gas flow process (cryogenic process). With the Bosch process, the "Teflon-like" layer must be etched from the bottom of the trench to continue etching. However with the cryogenic process we only deposit the passivation layer (thin oxide) on the sidewalls as continuous ion bombardment induces no passivation at the bottom of the trench. So we don't have the need to have very high ion bombardment in this case.

We would like to explicitly mention that these are preliminary results and that further work is ongoing.

3. Aspect ratio versus feature size

Fig. 3 shows a comparison of the aspect ratio versus feature size as studied by various groups [11–13,19–22] and updated here with our latest results. It appears that data pertaining to a particular etch process can follow a semi-empirical logarithmic law, which was previously reported for feature size in the tens of micrometer range [23] and which is found to still apply for the sub-micrometer range, considered in this paper:

$$AR = \frac{a\log(1+b.W)}{W} \quad (1)$$

where AR is the aspect ratio, W is width of the features (in μm), and a and b are constants with units of μm and μm^{-1}, respectively, that depend on the etching recipe being used. The aspect ratio is calculated as D/W, where D is the etch depth at the bottom of the trench. The best fit with this model was evaluated in five different cases and represented in Fig. 3. As it appears from the figure, the law applies over a wide dimension range. It can therefore be assumed that such trend lines can be used to reasonably predict the aspect ratios in ranges where experimental results are not available. In particular, by extrapolating the results to the limit of vanishing width W, the *ultimate* aspect ratio corresponding to a particular etching recipe can be evaluated:

$$\lim_{W\to 0} = \frac{a\log(1+b.W)}{W} = ab = AR_{max} \quad (2)$$

This ultimate aspect ratio can be calculated by performing experiments such as the Set 2 presented above, and can provide a dimension-less figure of merit (FOM = AR_{max}) for the effectiveness of a specific process to produce HAR sub-micrometer structures. For the cases analyzed in Fig. 2 we obtain the following FOM values: 3780 for our Set 2 process from Table 1, 3240, 180, 3000, and 168, respectively, for data previously reported in [11,12,21] and [22]. We can see that the FOM for [12] and [22] is significantly lower than the other processes, thus implying that these processes were not pushed until saturation to achieve the corresponding maximum aspect ratio features. A regression analysis was performed to assess the accuracy of the curve fits. The values of the regression coefficient r^2 attained for the above cases were above 0.96, with percentage errors for the a and b fit parameters calculated in the range of 7–9%, leading to an overall error on AR_{max} in the order of 15–20%. It must be noted that extending such trend-line extrapolation to dimensions above the micrometer range is not recommended, since most processes were optimized for the sub-micrometer range, and when applied to larger dimensions may result in dramatic undesired results such as the formation of silicon "grass".

4. Conclusions

Etching of sub-micrometer scale trenches was proven to give access to aspect ratios up to 124:1 and even 160:1, depending on the process parameters using both Bosch and cryogenic DRIE. A semi-empirical law relating aspect ratio to decreasing dimensions, and which takes into account the decrease in etch rate induced by radical and ion depletion, was experimentally validated at these scales. Furthermore, a figure of merit to evaluate the ultimate aspect ratio was proposed in the case of processes intended to achieve HAR features. The proposed figure of merit was applied to available experimental data from the literature.

References

[1] C.S. Song, Z.Y. Wang, Q.W. Chen, J. Cai, L.T. Liu, Microelectron. Eng. 85 (10) (2008) 1952–1956.
[2] M. Brunet, P. Dubreuil, H. Mahfoz-Kotb, A. Gouantes, A-M. Dorthe, Microsyst. Technol. 15 (9) (2009) 1449–1457.
[3] J.H. Klootwijk, K.B. Jinesh, W. Dekkers, J.F. Verhoeven, F.C. van den Heuvel, H.D. Kim, D. Blin, M.A. Verheijen, R.G.R. Weemaes, M. Kaiser, J.J.M. Ruigrok, F. Roozeboom, IEEE Electron Dev. Lett. 29 (7) (2008) 740–742.
[4] H. Berthet, J. Jundt, J. Durivault, B. Mercier, D. Angelescu, Lab Chip 11 (2) (2011) 215–223.
[5] B. Saadany, M. Malak, M. Kubota, F. Marty, Y. Mita, K. Diaa, T. Bourouina, IEEE J. Select. Top. Quant. Electron. 12 (6) (2006) 1480–1488.
[6] K. Termentzidis, J. Parasuraman, C. Abs da Cruz, S. Merabia, D. Angelescu, F. Marty, T. Bourouina, X. Kleber, P. Chantrenne, P. Basset, Nanoscale Res. Lett. 6 (2011) 288.
[7] S. Koynov, M.S. Brandt, M. Stutzmann, Appl. Phys. Lett. 88 (20) (2006) 203107.
[8] F. Larmer et al., Patents US 5501893 and EP 625285, 1996.
[9] S. Tachi, K. Tsujimoto, S. Okudaira, Appl. Phys. Lett. 52 (8) (1988) 616–618.
[10] F. Marty, L. Rousseau, B. Saadany, B. Mercier, O. Francais, Y. Mita, T. Bourouina, Microelectron. J. 36 (7) (2005) 673.
[11] K.J. Owen, B. Van Der Elzen, R.L. Peterson, K. Najafi, Proc. IEEE MEMS (2012) 251–254.
[12] R. Abdolvand, F. Ayazi, Sens. Actuat. A 144 (1) (2008) 109–116.
[13] W.J. Park, J.H. Kim, S.M. Cho, S.G. Yoon, S.J. Suh, D.H. Yoon, J. Surf. Coat. Tech. 171 (1-3) (2003) 290–295.
[14] T. Tillocher, W. Kafrouni, J. Ladroue, P. Lefaucheux, M. Boufnichel, P. Ranson, R. Dussart, J. Micromech. Microeng. 21 (2011) 085005.
[15] J.W. Coburn, H.F. Winters, Appl. Phys. Lett. 55 (26) (1989) 2730–2733.
[16] R.A. Gottscho, C.W. Jurgensen, J. Vitkavage, J. Vac. Sci. Technol. B 10 (1992) 2133.
[17] J. Yeom, Y. Wu, J.C. Selby, M.A. Shannon, J. Vac. Sci. Technol. B 23 (6) (2005) 2319–2329.
[18] Y. Mita, M. Kubota, M. Sugiyama, F. Marty, T. Bourouina, T. Shibata, in: Proc. IEEE MEMS Conf., Istanbul, Turkey, January 22–26, 2006, pp. 114–117.
[19] C.K. Chung, H.C. Lu, T.H. Jaw, Microsys. Tech. 16 (3) (2000) 106–108.
[20] A. Kok, T.-E. Hansen, T. Hansen, G.U. Jensen, N. Lietaer, M. Mielnik, P. Storas, in: IEEE Nuclear Sci. Symp. Conf. Rec., 2009, pp. 1623–1627.
[21] P. Basset, D. Galayko, A. Mahmood Paracha, F. Marty, A. Dudka, T. Bourouina, J. Micromech. Microeng. 19 (11) (2009) 115025.
[22] Y. Mita, K. Hirose, M. Kubota, T. Shibata, J. Sel. Top. Quant. Electron. 13 (2) (2007) 386–391.
[23] T. Bourouina, T. Masuzawa, H. Fujita, J. Microelectromech. Syst. 13 (2) (2004) 190–199.